

# Experimental Synchronization of two Integrated Multi-scroll Chaotic Oscillators

J.M. Muñoz-Pacheco<sup>\*1</sup>, E. Tlelo-Cuautle<sup>2</sup>, I. E. Flores-Tiro<sup>3</sup> and R. Trejo-Guerra<sup>4,2</sup>

<sup>1</sup> Facultad de Ciencias de la Electrónica  
Benemérita Universidad Autónoma de Puebla  
Puebla, Pue., México

\*jesum.pacheco@correo.buap.mx

<sup>2</sup> Departamento de Electrónica  
Instituto Nacional de Astrofísica, Óptica y Electrónica  
Tonantzintla, Pue., México

<sup>3</sup> Departamento de Ingeniería Electrónica y Telecomunicaciones  
Universidad Politécnica de Puebla  
San Mateo Cuanalá, Pue., México

<sup>4</sup> SEMTECH-Snowbush Mexico Design  
Aguascalientes, Ags., México

## ABSTRACT

Chaotic oscillators have been implemented with a wide variety of discrete electronic devices and quite few realizations using integrated circuit technology. This article describes the synchronization of two chaotic oscillators already fabricated with complementary metal-oxide-semiconductor (CMOS) integrated circuit technology of 0.5 $\mu$ m and generating 3- and 5-scrolls. In order to attain the synchronization, we use a master-slave topology with unidirectional coupling. Within this context, a system parameter iterates until the correlation coefficient computed between the chaotic signals generated by the master and slave systems approximates to unity. For the following parameter, its value depends on the standard deviations from the individual signals contrary to previous one. By combining those statistical relationships according to the number of system parameters, we can synchronize integrated chaotic oscillators. Theoretical model simulations of two chaotic oscillators generating 3- and 5-scrolls, and experimental results for two integrated 3-scroll chaotic oscillators validate this approach. Stability and error analysis are also included.

Keywords: Chaos, Synchronization, Integrated Circuit, CMOS, Multi-scroll.

## RESUMEN

Los osciladores caóticos se han implementado con una variedad amplia de dispositivos electrónicos discretos y muy pocos con tecnología de circuitos integrados. Este artículo describe la sincronización de dos osciladores caóticos fabricados con tecnología de circuitos integrados CMOS de 0.5 $\mu$ m que generan 3- y 5-enrollamientos. Se utiliza la configuración maestro-esclavo para obtener la sincronización. A partir de esta configuración, se itera un parámetro del sistema hasta que el coeficiente de correlación entre las señales caóticas del maestro y el esclavo respectivamente, se aproxima a la unidad. Posteriormente, se calcula la razón de las desviaciones estándar para obtener el valor del siguiente parámetro, esto de forma inversa a la determinación del primero. Es posible sincronizar osciladores caóticos integrados al combinar estas medidas estadísticas en relación al número de parámetros del sistema. Simulaciones del modelo teórico de dos osciladores caóticos exhibiendo tres y cinco enrollamientos, además de resultados experimentales para tres enrollamientos confirman el método propuesto. Son incluidos los análisis de error y estabilidad.

## 1. Introduction

Carroll and Pecora verified the experimental synchronization of two chaotic oscillators by using operational amplifiers (opamps) [1]. They pointed out that if two independent chaotic systems were started with the same initial conditions, any

arbitrarily small perturbation in those conditions would grow exponentially. After some time, the trajectory evolution of the two systems will be uncorrelated. However, if the two chaotic oscillators were synchronized, both systems will

evolve to the same chaotic behavior, e.g., in a master-slave topology [2-6], the slave system behaves as the master system despite their chaotic motion, provided they are both driven with a proper signal. In this manner, the general scheme for synchronizing dynamical systems is to take a (nonlinear) system, duplicate some sub-system of that system and drive it with a control signal from the unduplicated part. This is a self-synchronization where the two sub-systems couples by some technique [1-6], [13]. As a function of the synchronized states, we can classify the synchronization approaches as complete synchronization, phase synchronization, lag and intermittent lag synchronization, imperfect phase synchronization, and almost synchronization [14-17, 20-26]. However, those approaches have been generally proved on chaotic systems depicted by either theoretical relationships or electronic circuits designed with discrete devices opposed to the integrated circuit (IC) case [2-6].

Related to multi-scroll chaotic oscillators, they have been implemented using several approaches, such as opamps, operational transconductance amplifiers (OTAs), and current-feedback opamps (CFOAs) [7]. Note that by interconnecting and superimposing unity-gain cells (UGCs) [8-9], one could design those active devices with complementary metal-oxide-semiconductor CMOS IC technology. This approach was previously reported in [10-11], demonstrating that chaotic oscillators can be realized with IC technology. An integrated chaotic oscillator provides key advantages such as; it reduces the form factor (passive and active device count) contrary to the discrete realizations, and the bandwidth of the chaotic signals increases as a function of the time-constants that can be reached with different IC fabrication technologies.

This issue is quite important in an actual encryption scheme based on chaos, which needs high-rate data transmission, as mentioned in [14]. Finally, having ICs one can tune or select the chaotic behavior using a few external passive elements or exploiting the programming capabilities of current mirrors or logic gates. Another advantage in having integrated chaotic oscillators, is that one can develop custom designs that can derive in realizing custom synchronization approaches, thus allowing to realize integrated

designs for communication systems, which are in the state-of-the-art [21-24].

In this manner, to the best of our knowledge, this paper is the first one reporting a systematized algorithm to synchronize two chaotic oscillators at integrated circuit level. The novel contribution to the field consists on a systematic algorithm to synchronize integrated chaotic systems with multiple scrolls by using the correlation coefficient (CoCo) and standard deviation (STD) of the numerical time series to reduce the synchronization error iteratively. Besides, the stability conditions are based on conditional Lyapunov exponents computed only once before the first iteration. Therefore, the synchronization is achieved no matter the values of the initial conditions in the synchronization scheme. This approach can be considered as an extension of the complete synchronization technique based on unidirectional coupling [2, 6, 13].

The main idea of this method consists on sending a chaotic signal from the integrated nonlinear system (master) to another (slave). Then, the slaved system tracks the dynamics of the master system. This means that the behavior of the second system does not have any influence on the first one. Additionally, a 45-degree straight line, on the phase space portrait, is a well-accepted criterion to confirm the synchronization. This results when the same state-variables taken from the integrated master and slave dynamical systems are compared. Note that the dynamical evolution of the chaotic signals is theoretically identical after the synchronization is attained. Within this context, we computed CoCo between the time series of both the master and slave systems. When the data are correlated, the synchronization can be ensured. In a similar way, we used STD of independent chaotic signals to verify the synchronization error, i.e., when this measure converges to the same value implies that chaotic signals are close related and synchronized. Additionally, we can adjust a positive lineal approximation for both statistical measures by varying the parameters in the slave system. It is also proved that this approach is asymptotically stable by computing the conditional Lyapunov exponents. Several numerical simulation results for 3- and 5-scroll chaotic attractors confirm the synchronization approach. Finally, experimental

results for two 3-scroll integrated chaotic oscillators are also shown.

### 2. Integrated chaotic oscillator

Recently, a modified Chua's system was designed and fabricated with CMOS IC technology of 0.5um [10-11]. That IC can generate 3- and 5-scrolls, and its chaotic behavior was demonstrated by computing the maximum Lyapunov exponent [12].

We take that chip as the core of chaotic behavior for our approach. Therefore, the dynamics of the Chua's system is governed by

$$\begin{aligned} \dot{x}_1 &= \alpha x_2 + f(x_1) \\ \dot{x}_2 &= \alpha x_1 - \gamma x_2 - \alpha x_3 \\ \dot{x}_3 &= \beta x_2, \end{aligned} \tag{1}$$

being  $[\alpha, \beta, \gamma]$  constant parameters,  $x_1, x_2, x_3$  the state-variables, and  $f(x_1)$  a nonlinear function approximated by

$$\begin{aligned} f(x_1) &= \begin{cases} -\xi(x_1 / B_p), \\ \xi[2k\text{sgn}(x_1 / B_p) - x_1 / B_p], \end{cases} \\ &|x_1| \leq B_p \\ &|x_1| \leq B_p(2k+1) \ \& \ |x_1| > B_p(2k-1) \end{aligned} \tag{2}$$

for 3-scrolls case, and

$$\begin{aligned} f(x_1) &= \begin{cases} -\xi(x_1 / B_p), \\ \xi[2k\text{sgn}(x_1 / B_p) - x_1 / B_p], \\ \xi[4k\text{sgn}(x_1 / B_p) - x_1 / B_p], \end{cases} \\ &|x_1| \leq B_p \\ &|x_1| \leq B_p(2k+1) \ \& \ |x_1| > B_p(2k-1) \\ &|x_1| \leq B_p(2k+1) \ \|\ |x_1| > B_p(2k-1) \end{aligned} \tag{3}$$

for 5-scrolls case, where  $\xi$  defines the dynamic range of the sawtooth function,  $B_p$  are the breakpoints and  $k$  is a multiplier factor. By

selecting  $\alpha=3, \beta=4, \gamma=1, \xi=0.8 \text{ V}, B_p=147 \text{ mV}$ , and  $k=1$ ; the chaotic behavior arises [3].

Basically, the integrated chaotic oscillator consists of UGCs like, voltage followers (VFs), current followers (CFs) and current mirrors (CMs), as shown in Fig. 1.

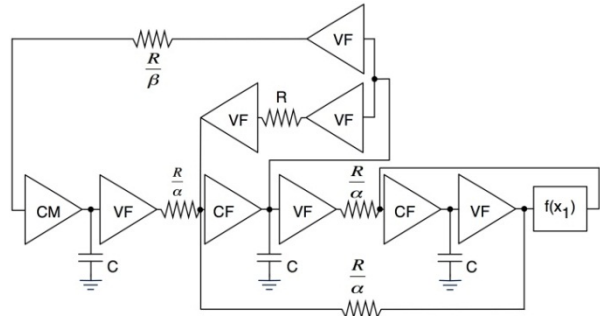


Figure 1. Integrated chaotic oscillator taken from [10-11].

All those UGCs were designed using floating gate MOS (FGMOS) transistors [10-11]. From Figure 1,  $R$  and  $C$  define the gain of the integrator blocks ( $\tau=t/RC$ ); with  $R=120\text{k}\Omega$  and  $C$  chosen according to the desired operating frequency. Note that  $C$  is the sum of the external capacitance plus the parasitic capacitance [10]. As the integration is performed externally, we can add a control signal, with a proper impedance coupling, to the slave system; e.g., using opamps as shown herein. This signal could be injected as a current at the nodes connecting the integration capacitors ( $C$ ). Therefore, the gain of the opamp must be equal to  $1/R$  and multiplied by the gain of the signal to be transmitted. A chip microphotograph is shown in [10].

### 3. Synchronization of integrated multi-scroll chaotic oscillators

It is well known that the Pearson CoCo measures the strength and direction of a linear relationship between two variables. As this coefficient approaches unity, we can state that the chaotic signals of master and slave systems have a strong positive correlation, and so are synchronized. The STD was computed to compare two chaotic signals. If the signals from the master and slave are synchronized, we expect that they have the same STD. Synchronization error being minimized when both statistical measures approach unity.

Taken into account those concepts, this section presents the synchronization method for integrated chaotic systems. The proposed approach could be considered as enhanced version of paper in [13]. From the chaotic system described by (1), we select to be the master state controlling the dynamics of the slave system. That way, the slave system becomes

$$\begin{aligned}\dot{y}_1 &= ay_2 + f(x_1) \\ \dot{y}_2 &= ax_1 - cy_2 - ay_3 \\ \dot{y}_3 &= by_2,\end{aligned}\quad (4)$$

The values for  $[a, b, c]$  are randomly selected at the beginning of our approach. A significant remark is that the behavior of the sub-system  $[y_2, y_3]$ , depends on  $x_1$ ; nevertheless the behavior of  $x_1$  is not influenced by  $[y_2, y_3]$ . We select  $x_1$  as the driving signal because the resulting conditional Lyapunov exponents have a negative magnitude [14]. This is a necessary and sufficient condition for the integrated chaotic oscillators to be synchronized, as shown herein.

### 3.1 Synchronization conditions: Conditional Lyapunov exponents

Let us consider a state-variable subsystem defined by

$$\dot{v}' = \dot{v} - \hat{v} \quad (5)$$

where  $v$  represents the state variables  $[x_2, x_3]$  of the master integrated chaotic system, and  $\hat{v}$  the state-variables of the slave  $[y_2, y_3]$ . By integrating (5), we have

$$v = v - \hat{v} = \begin{bmatrix} v'_2 \\ v'_3 \end{bmatrix} = \begin{bmatrix} x_2 - y_2 \\ x_3 - y_3 \end{bmatrix} \quad (6)$$

and the differentiation of  $v$  and  $\hat{v}$ , according to (1) and (4) becomes

$$\dot{v}' = \begin{bmatrix} \dot{x}_2 \\ \dot{x}_3 \end{bmatrix} = \begin{bmatrix} -\gamma & -\alpha \\ \beta & 0 \end{bmatrix} \begin{bmatrix} x_2 \\ x_3 \end{bmatrix} \quad (7)$$

$$\dot{\hat{v}} = \begin{bmatrix} \dot{y}_2 \\ \dot{y}_3 \end{bmatrix} = \begin{bmatrix} -\gamma & -\alpha \\ \beta & 0 \end{bmatrix} \begin{bmatrix} y_2 \\ y_3 \end{bmatrix} \quad (8)$$

By substituting (6), (7) and (8) in (5), we obtain

$$\dot{v}' = \begin{bmatrix} -\gamma & -\alpha \\ \beta & 0 \end{bmatrix} \begin{bmatrix} v'_2 \\ v'_3 \end{bmatrix} = P \begin{bmatrix} v'_2 \\ v'_3 \end{bmatrix} \quad (9)$$

This subsystem represents the dissipative part of the modified Chua's system in (1). It is known that if matrix  $P$  has a pair of complex conjugated roots with negative real parts, the synchronization error is asymptotically stable [14]. For our case, the eigenvalues of the matrix  $P$  are  $\lambda_{c_{1,2}} = -0.5 \pm 3.4j$ .

Thus, all conditional Lyapunov exponents of integrated chaotic oscillators must be negative to guarantee the synchronization. Note that the maximum Lyapunov exponent remains being positive in order to generate chaotic behavior.

### 3.2 Synchronization conditions: Error analysis

This subsection shows that the synchronization error minimizes (it converges to zero ideally) as time tends towards infinity. Let us define the state errors for the master and slave systems as  $e_1 = x_1 - y_1$ ,  $e_2 = x_2 - y_2$  and  $e_3 = x_3 - y_3$ . By using (1) and (4), and considering that  $\alpha = a$ , it leads us to

$$\begin{aligned}\dot{e}_1 &= \dot{x}_1 - \dot{y}_1 = (\alpha x_2 + f(x_1)) - (\alpha y_2 + f(x_1)), \\ \dot{e}_2 &= \alpha x_2 - \alpha y_2 = \alpha e_2.\end{aligned}\quad (10)$$

If the synchronization error  $e_1$  is designed to vanish gradually, then its differentiation is  $\dot{e}_1 \rightarrow 0$  in (10). This means that the synchronization error  $e_2$  tends to zero in order to accomplish this equality. As a result,  $e_2 \rightarrow 0$  and  $\dot{e}_2 \rightarrow 0$ .

Therefore, we have the following expression for the synchronization error  $\dot{e}_2$ .

$$\begin{aligned}\dot{e}_2 &= \dot{x}_2 - \dot{y}_2 = (\alpha x_1 - \gamma x_2 - \alpha x_3) - (\alpha x_1 - \gamma y_2 - \alpha y_3) \\ \dot{e}_2 &= -\gamma e_2 - \alpha e_3 \\ 0 &= -\alpha e_3, e_3 \rightarrow 0, \dot{e}_3 \rightarrow 0\end{aligned}\quad (11)$$

with  $c = \gamma$ . Finally, the synchronization error  $\dot{e}_3$  implies that  $b = \beta$  as follows

$$\begin{aligned} \dot{e}_3 &= \dot{x}_3 - \dot{y}_3 = \beta x_2 - \beta y_2 \\ \dot{e}_3 &= \beta e_2 \\ 0 &= \beta e_2 \end{aligned} \tag{12}$$

That way, since  $e_1$  tends towards zero, then  $e_2 \approx 0$  and  $e_3 \approx 0$  does. The previous analysis, although intuitive, is linked to a rigorous mathematical treatment based on the idea that the synchronization of entire coupled chaotic systems can be realized by synchronizing only partial states of that chaotic systems [14-15].

### 3.3 Systematic approach to synchronize integrated chaotic systems

In the context of synchronization, a key remark is that matrix  $P$  representing the dissipative part of the integrated chaotic oscillators must have negative conditional Lyapunov exponents with form of  $\lambda c_{1,2} - \Sigma \pm j\Omega$ . Therefore, neither the same initial conditions nor belong to the same attraction region are required. Thus we propose that by giving an integrated nonlinear chaotic system  $\dot{x} = f(x)$ , with parameters  $m$ ,  $m \in \mathfrak{R}$ ; we can determine the signal from the master to control the slave system only if this satisfies the necessary and sufficient condition in (9).

Once the output has been decided, the parameters of the slave system are swept linearly in the interval  $\Psi = \{m, m \in \mathfrak{R} : \min < m < \max\}$ , being  $\min$  and  $\max$ , the minimal and maximum values where the chaotic regime remains. For the first parameter, the CoCo is computed until  $\rho x_i y_i \approx 1$ . Similarly, for the second parameter, the SDT is obtained until  $\sigma x_i / \sigma y_i \approx 1$ . The resolution for each parameter can be adjusted by increasing the number of iterations of CoCo and STD.

Both statistical measures are intercalated for the remaining parameters. By satisfying (10), (11), (12), we obtains  $\lim_{t \rightarrow \infty} \epsilon(t) = x(t) - y(t) = 0$ . In this manner, an algorithm with five iterative steps is summarized herein:

-Step. Considering  $\alpha = 3$ ,  $\beta = 4$ ,  $\gamma = 1$  in the master chaotic oscillator, choose a random value for the parameters  $(a, b, c)$  of the slave system.

-Step 2. Letting  $(b, c)$  fixed, compute the solution of (1) and (4) simultaneously while  $a$  is being modified each cycle until the CoCo between the numerical time series approximates to unity, i.e.,

$$\rho x_i y_i = \frac{\sigma x_i y_i}{\sigma x_i \sigma y_i} \approx 1$$

-Step 3. Set the best value for  $a$  from the previous step and letting now  $(a, c)$  fixed, compute the solution of (1) and (4) simultaneously while  $b$  is being modified each cycle until the rate of STD of the numerical time series approximates unity, i.e.,

$$\frac{\sigma x_i}{\sigma y_i} = \sqrt{\frac{1}{N} \sum_{j=1}^N ((x_i)_j - \bar{x}_i)^2} / \sqrt{\frac{1}{N} \sum_{j=1}^N ((y_i)_j - \bar{y}_i)^2} \approx 1$$

-Step 4: Similarly, setting the best value for  $(a, b)$ , compute the solution of (1) and (4) simultaneously while  $c$  is being modified each cycle until the CoCo between the numerical time series approximates to unity, i.e.,  $\rho x_i y_i = \frac{\sigma x_i y_i}{\sigma x_i \sigma y_i} \approx 1$ .

-Step 5. If the precision of the CoCo and STD does not meet with the required specifications, use the best values found for  $(a, b, c)$  and repeat the algorithm. This is considered as a *round*.

## 4. Numerical Simulation Results

By using the aforementioned algorithm, we synchronize the integrated chaotic attractors in (1) and (4) with  $(x_1, x_2, x_3) = (0.1, 0, 0)$  and  $(y_1, y_2, y_3) = (0.01, 0, 0)$  as initial conditions, respectively. The computation of the first rounds to generate 3- and 5-scrolls is shown in Tables 1, 2 and 3. In this work, we complete ten *cycles* for each one of parameters  $(a, b, c)$  using the Adams-Moulton algorithm with a step-size  $h = 0.01$  as numerical solver [18]. The vectors containing the time series have a length of 10000 *data*, which is equivalent to be considered as a long-term

evolution; a necessary condition to capture the chaotic behavior of those systems [14]. Those values (*cycles* and *data*) can be increased as needed for the user; however, it could be a negative impact in the simulation time [19].

It is significant to observe from Tables 1 and 2 that the values for the parameters (*a, b, c*) are chosen with more digits as the number of cycles increases.

This is related to the required precision for the CoCo and STD in order to satisfy the

synchronization error in (10), (11) and (12). As a function of the synchronized states, we search for the best values for the parameters.

After five rounds, we found  $(a, b, c) = (3.17, 4.23, 1.12)$ , which are quite similar as the ones used in references [10-11] for (1), where  $(\alpha, \beta, \gamma) = (3, 4, 1)$ . To generate 5-scrolls, the values computed after five cycles were  $(a, b, c) = (2.90, 3.99, 0.88)$  as given in Table 3. In addition, by using the ideal values  $(\alpha, \beta, \gamma) = (3, 4, 1)$  in both the master and slave systems, the CoCo and STD are given in Tables 4 and 5.

cycle	a	b	c	$\rho x1y1$	cycle	a	b	c	$\sigma x1/\sigma y1$	cycle	a	b	c	$\rho x1y1$
1	3	4	1	0.999690191	1	3.101	4	1	0.97751545	1	3.101	4.099	1	0.998181139
2	3.1	4	1	0.999840239	2	3.101	4.1	1	1.00076492	2	3.101	4.099	1.1	0.997932578
3	3.2	4	1	0.998969017	3	3.101	4.11	1	1.00301881	3	3.101	4.099	1.01	0.998235132
4	3.21	4	1	0.998843093	4	3.101	4.101	1	1.00099088	4	3.101	4.099	1.05	0.998273115
5	3.11	4	1	0.999795253	5	3.101	4.105	1	1.00189345	5	3.101	4.099	1.09	0.998034267
6	3.15	4	1	0.999504205	6	3.101	4.09	1	0.998498309	6	3.101	4.099	0.9	0.996619562
7	3.12	4	1	0.999735669	7	3.101	4.099	1	1.00023883	7	3.101	4.099	1.12	0.997680056
8	3.13	4	1	0.999666984	8	3.101	4.095	1	0.999633209	8	3.101	4.099	1.02	0.998271164
9	3.101	4	1	0.999840687	9	3.101	4.01	1	0.979899498	9	3.101	4.099	1.075	0.998155588
10	3.111	4	1	0.999789719	10	3.101	4.12	1	1.00526005	10	3.101	4.099	1.081	0.998111584

Table 1. Computing the best values (*a, b, c*) to generate 3-scrolls (round=1).

cycle	a	b	c	$\rho x1y1$	cycle	a	b	c	$\sigma x1/\sigma y1$	cycle	a	b	c	$\rho x1y1$
1	3.101	4.099	1.05	0.998273115	1	2.989	4.099	1.05	1.04527827	1	2.989	3.919	1.05	0.996647785
2	3.001	4.099	1.05	0.998964468	2	2.989	3.999	1.05	1.02181217	2	2.989	3.919	1.1	0.995180368
3	3.005	4.099	1.05	0.998957072	3	2.989	3.99	1.05	1.01962827	3	2.989	3.919	0.999	0.997626434
4	2.99	4.099	1.05	0.998974210	4	2.989	4	1.05	1.02205408	4	2.989	3.919	1	0.997612520
5	2.999	4.099	1.05	0.998967412	5	2.989	4.01	1.05	1.02446504	5	2.989	3.919	0.99	0.997741899
6	3	4.099	1.05	0.998966004	6	2.989	3.89	1.05	0.994543691	6	2.989	3.919	0.9	0.997888097
7	2.991	4.099	1.05	0.998974033	7	2.989	3.899	1.05	0.996863328	7	2.989	3.919	0.91	0.997965728
8	2.98	4.099	1.05	0.998969171	8	2.989	3.9	1.05	0.997120307	8	2.989	3.919	0.92	0.998019246
9	2.989	4.099	1.05	0.998974373	9	2.989	3.95	1.05	1.00977557	9	2.989	3.919	0.95	0.998037860
10	2.9891	4.099	1.05	0.998974362	10	2.989	3.919	1.05	1.00197396	10	2.989	3.919	0.951	0.998034872

Table 2. Computing the best values (*a, b, c*) to generate 3-scrolls (round=2).

cycle	a	b	c	$\rho x_1 y_1$	cycle	a	b	c	$\sigma x_1 / \sigma y_1$	cycle	a	b	c	$\rho x_1 y_1$
1	2.97	4.025	0.91	0.998664638	1	2.9	4.025	0.91	1.00767485	1	2.9	3.99	0.91	0.999533088
2	2.98	4.025	0.91	0.998552665	2	2.9	4	0.91	1.00270091	2	2.9	3.99	0.9	0.999591084
3	2.975	4.025	0.91	0.998609587	3	2.9	3.99	0.91	1.00068775	3	2.9	3.99	0.95	0.999104651
4	2.96	4.025	0.91	0.998768871	4	2.9	3.8	0.91	0.959709635	4	2.9	3.99	0.99	0.998378664
5	2.95	4.025	0.91	0.998864832	5	2.9	3.9	0.91	0.981940075	5	2.9	3.99	0.89	0.999628735
6	2.94	4.025	0.91	0.998951961	6	2.9	3.91	0.91	0.984080496	6	2.9	3.99	0.8	0.998994565
7	2.93	4.025	0.91	0.999029672	7	2.9	3.93	0.91	0.988317633	7	2.9	3.99	0.895	0.999612474
8	2.92	4.025	0.91	0.999097350	8	2.9	3.95	0.91	0.992497265	8	2.9	3.99	0.891	0.999625895
9	2.9	4.025	0.91	0.999199909	9	2.9	3.97	0.91	0.996620319	9	2.9	3.99	0.889	0.999631367
10	2.91	4.025	0.91	0.999154351	10	2.9	3.98	0.91	0.998660927	10	2.9	3.99	0.88	0.999645690

Table 3. Computing the best values (a, b, c) to generate 5-scrolls (round=5).

From Tables 4 and 5, we observe that the behavior between the numerical time series continues similar although the high-resolution is a few lost. For the case under study, this fact does not matter because we can adapt those relationships using some external electronic device as will be shown in the next section.

In Figure 2, we show the 3-scroll chaotic attractors of the master and slave systems already synchronized. Additionally, Figure 3(a) shows the time evolution of the state-variables  $(x_1, y_1)$ .

Considering that this simulation was computed using the normalized Chua's system, we obtain the synchronization after 20 seconds. Also, the synchronization error for this case is shown in Figure 3(b), where its magnitude is suitable. Related to 5-scrolls case, Figure 4(a) shows its chaotic attractor.

Figures 4(b), 4(c) and 4(d) show the synchronization in the phase space for  $(x_1, y_1)$ ,  $(x_2, y_2)$  and  $(x_3, y_3)$ , respectively.

A straight line on those phase space diagrams represents a minimum synchronization error. Therefore, our algorithm is appropriate to synchronize integrated chaotic systems as previously shown.

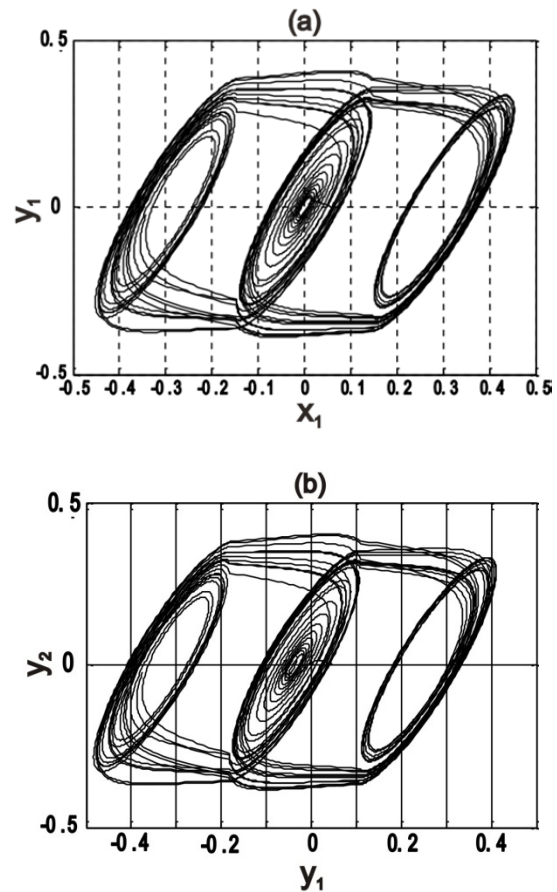


Figure 2. 3-scroll attractor; (a) Master, (b) slave.

### 5. Experimental Realization

The experimental results of synchronizing two double scroll Chua's chaotic oscillators were given in [2], but by using the commercially available CFOA AD844 in CCII+ configuration. Contrary to that, in this section we show the synchronization results using the IC introduced in [10-11] for the case with 3-scrolls.

a	b	c	$\rho x_1 y_1$	$\sigma x_1 / \sigma y_1$
3	4	1	0.9999949635	1.01237867

Table 4. CoCo and STD to generate 3-scrolls.

a	b	c	$\rho x_1 y_1$	$\sigma x_1 / \sigma y_1$
3	4	1	0.9999962877	0.999963232

Table 5. CoCo and STD to generate 5-scrolls.

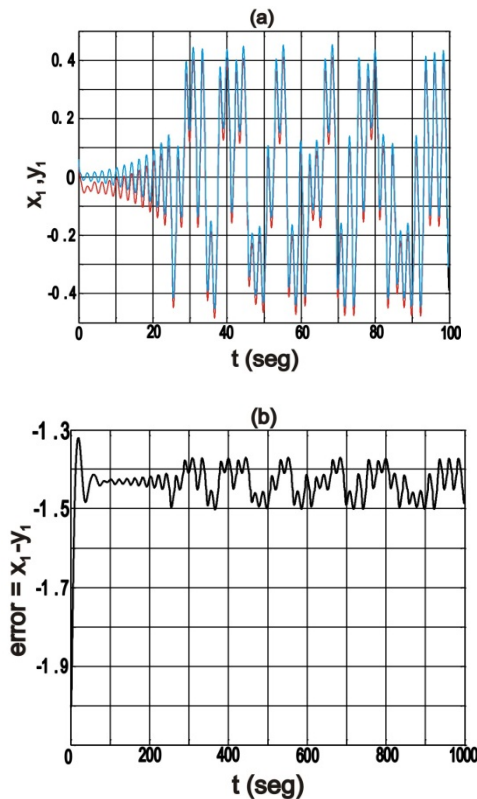


Figure 3. (a) Time synchronization between  $(x_1, y_1)$ , (b) Logarithmic synchronization error.

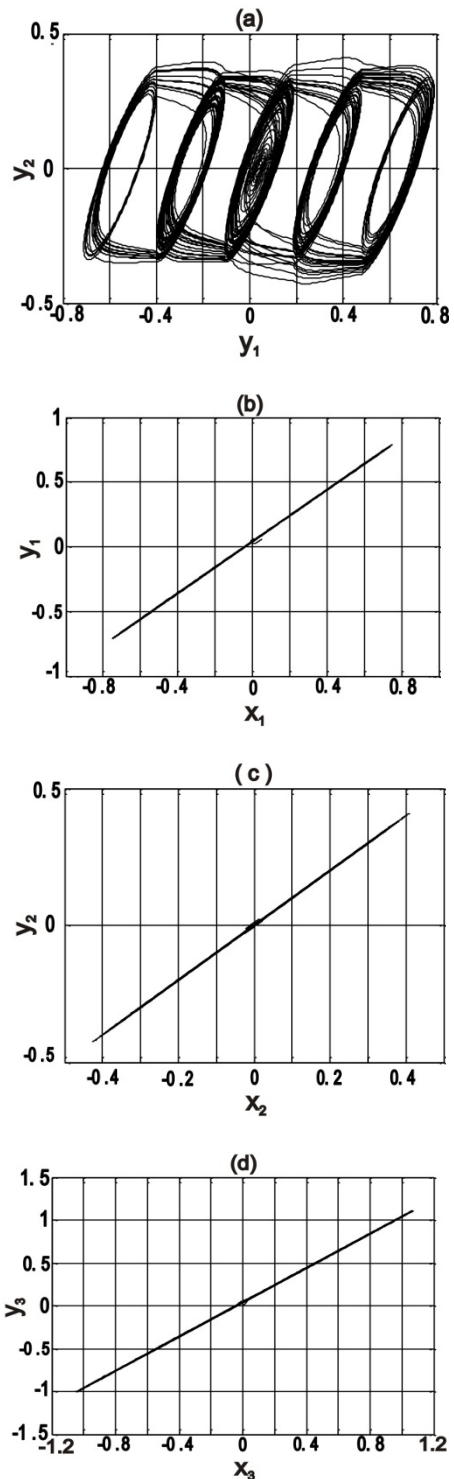


Figure 4. (a) 5-scroll chaotic attractor; (b), (c), (d) Phase diagrams verifying the master-slave synchronization for 5-scrolls case.



Henceforth, we propose the experimental setup of the synchronization approach as shown in Figure 5. The values of the external elements, as well as the chip pinouts, are setting as given in [10-11]. As was demonstrated in section 3, the synchronization error is asymptotically stable when the nonlinear function of the slave-system is controlled directly by a state from the master. According to that, we take from an integrated analog output buffer, a sample of the chaotic signal of the state  $x_1$  (master) marked in Figure 5. Note that this output controls the nonlinear function of slave system  $f(y_1)$ .

The differential amplifier compares the voltages generated from states  $x_1$  and  $y_1$ . This difference is injected as a current by the voltage-to-current converter resistor at the bidirectional current pin of the integration capacitor  $C_1$ . This means that the voltage variation in the integration capacitor at the slave system depends on two voltages, one from itself and another from the master system. In this manner, the synchronization is possible when the error  $(x_1 - y_1)$  tends towards zero as the feedback current reduces. Figure 6 shows two states  $(x_1, x_2)$  of the master system and their chaotic attractor.

Figure 7 shows the states  $(x_1, y_1)$  and  $(x_2, y_2)$ , respectively. Finally, the phase space diagram for  $(x_2, y_2)$  and its synchronization noise are shown in Figure 8.

From those experimental results, we observe a suitable synchronization because of the synchronization error agrees with (10), (11) and (12). At experimental level, the noise-level of the reported synchronization scheme is negligible (<5mv); which is suitable for voltage-mode signal processing of several engineering applications.

### 6. Conclusion

We showed the synchronization of two multi-scroll chaotic oscillators by applying a straightforward method [13]. Contrary to traditional methods, it was demonstrated that the proposed approach is useful to synchronize integrated chaotic systems if the conditional Lyapunov exponents have negative real parts. Therefore, the synchronization is achieved no matter the values for the initial conditions of the synchronization scheme. The synchronization approach was based on a master-slave topology with unidirectional coupling.

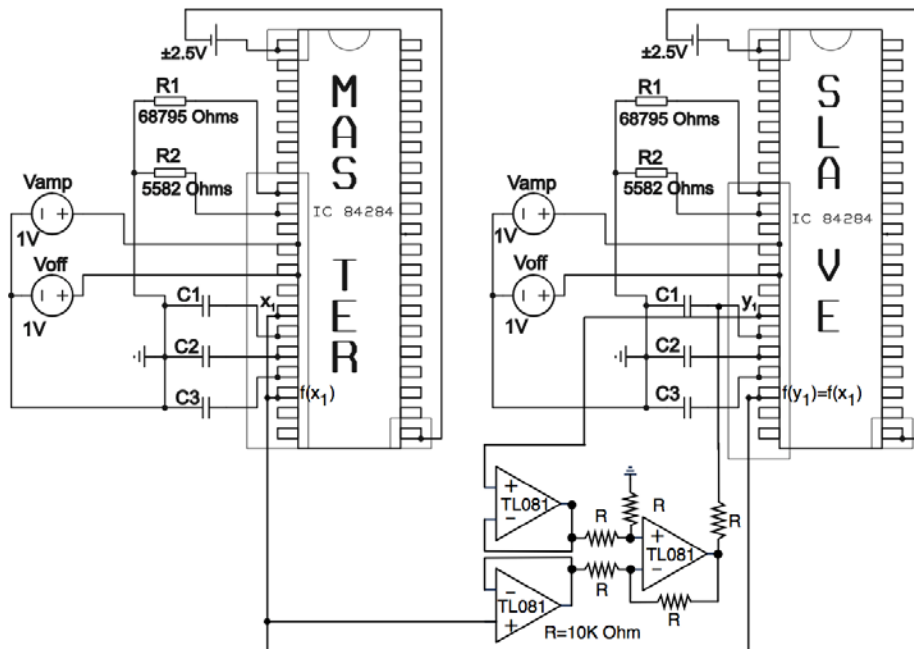


Figure 5. Experimental set-up for the synchronization between two integrated modified Chua's oscillators.

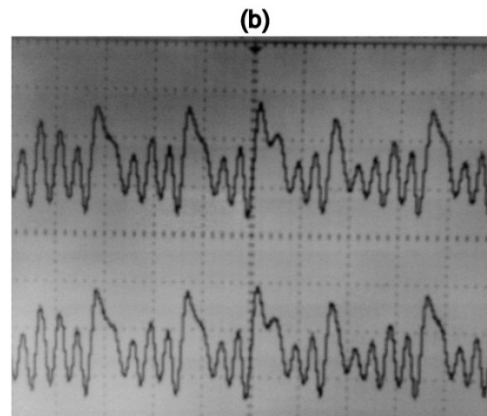
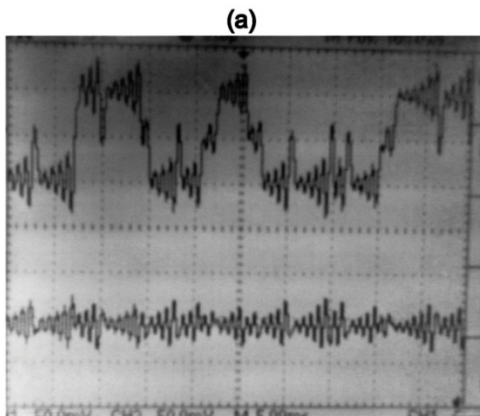


Figure 7. (a) States  $(x_1, y_1)$  of the master (up) and slave (down), and (b) states  $(x_2, y_2)$  of the master (up) and slave (down), respectively, with 50mV/div.

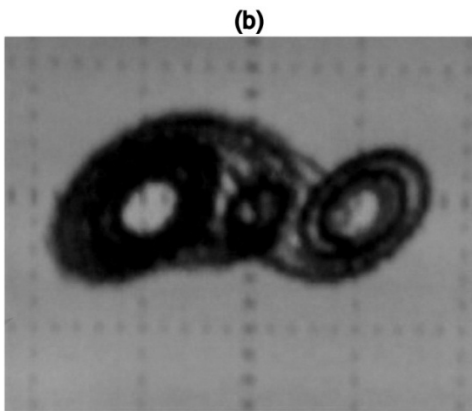


Figure 6. (a) Master states  $(x_1, x_2)$ , and (b) their phase diagram with 50 mV/div.

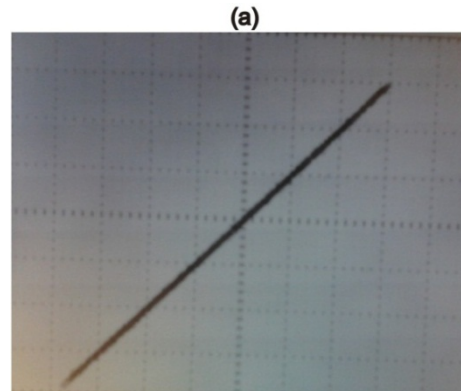
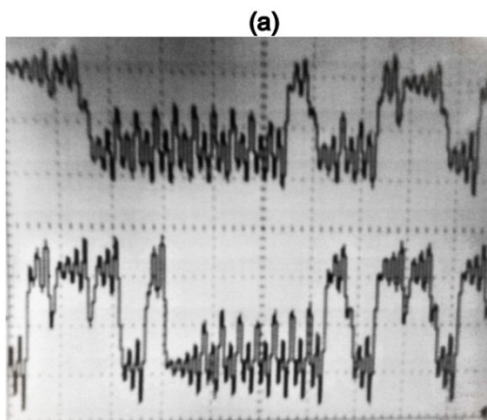


Figure 8. Figure 8. (a) Phase diagram for the synchronization of Figure 7(b) with 20mV/div, (b) Synchronization noise between master and slave systems with 50mV/div.

The optimal parameters for the synchronization were found from the correlation coefficient and standard deviations computed between the chaotic signals generated by the master and slave systems. Although using a low-resolution for those statistical measures, we found that the synchronization is possible. This is vital because integrated circuits can have variations that could alter the ideal values of system parameters causing losing the synchronization. The numerical simulation results were presented for the chaotic oscillators generating 3- and 5-scrolls, while the experimental results were presented for the chaotic oscillators generating 3-scrolls. In this last case, we used the IC already designed and fabricated with technology of 0.5 $\mu$ m of [10-11]. Both, the numerical simulations and the experimental results show a correct synchronization between two integrated chaotic oscillators.

#### Acknowledgements

This work has been partially supported by SEP PROMEP and VIEP-BUAP under Projects BUAP-PTC-359 and 2014-VIEP Grants, respectively.

The authors would like to gratefully acknowledge CONACyT for the support under grant 131839-Y.

#### References

- [1] T.L. Carroll and L.M. Pecora, "Synchronizing Chaotic Circuits," *IEEE Trans. Circuits Syst.*, vol. 38, no. 4, pp. 453-456, April 1991.
- [2] R. Trejo-Guerra et al., "Chaotic communication system using Chua's oscillators realized with CCII+s," *Int. J. of Bifurc. Chaos*, vol. 19, no. 12, pp. 4217-4226, 2009.
- [3] L. Gámez-Guzmán et al., "Synchronization of multi-scroll chaos generators: application to private communication," *Rev. Mex. Fis.*, vol. 54, no. 4, pp. 299-305, 2008.
- [4] J.L. Mata-Machuca et al., "Chaotic Systems Synchronization Via High Order Observer Design," *J. Appl. Res. Technol.*, vol. 9, no. 1, pp. 57-68, 2011.
- [5] X. Zhang et al., "Synchronization for Time-Delay Lur'e Systems with Sector and Slope Restricted Nonlinearities Under Communication Constraints," *Circuits Syst. Signal Pr.*, vol. 30, no. 6, pp. 1573-1593, 2011.
- [6] J.M. Muñoz-Pacheco et al., "Synchronization of PWL function-based 2D and 3D multi-scroll chaotic systems," *Nonlinear Dyn.*, vol. 70, no. 2, pp. 1633-1643, 2012.
- [7] J.M. Muñoz-Pacheco et al., "OpAmp-, CFOA- and OTA-Based Configurations to Design Multi-Scroll Chaotic Oscillators," *Trends Appl. Sci. Res.*, vol. 7, no. 2, pp. 168-174, 2012.
- [8] M.A. Duarte-Villaseñor et al., "Binary genetic encoding for the synthesis of mixed-mode circuit topologies," *Circuits Syst. Signal Pr.*, vol. 31, no. 3, pp. 849-863, 2012.
- [9] C. Sanchez-Lopez, "A 1.7 MHz Chua's circuit using VMs and CF+s," *Rev. Mex. Fis.*, vol. 58, no. 1, pp. 86-93, 2012.
- [10] R. Trejo-Guerra et al., "Multiscroll Floating Gate Based Integrated Chaotic Oscillator," *Int. J. Circuit Theory Appl.*, vol. 41, no. 8, pp. 831-843, 2013.
- [11] R. Trejo-Guerra et al., "Integrated Circuit Generating 3- and 5-Scroll Attractors," *Commun. Nonlinear Sci. and Numer. Simul.*, vol. 17, no. 11, pp. 4328-4335, 2012.
- [12] L.G. de la Fraga et al., "On Maximizing Positive Lyapunov Exponents in a Chaotic Oscillator with Heuristics," *Rev. Mex. Fis.*, vol. 58, no. 3, pp. 274-281, 2012.
- [13] J.P. Yeh and K.L. Wu, "A simple method to synchronize chaotic systems and its application to secure communications," *Math. Comput. Model.*, vol. 47, no. 9-10, pp. 894-902, 2008.
- [14] B. Jovic, "Synchronization Techniques for Chaotic Communication Systems," Berlin, Germany: Springer-Verlag, 2011.
- [15] J.J.E. Slotine and W. Li, "Applied Nonlinear Control," Englewood Cliffs, NJ: Prentice-Hall, 1993.
- [16] C. Posadas-Castillo et al., "Experimental realization of binary signals transmission based on synchronized Lorenz circuits," *J. Appl. Res. Technol.*, vol. 2, no. 2, pp. 127-137, 2004.
- [17] H. Serrano-Guerrero et al., "Chaotic synchronization in nearest-neighbor coupled networks of 3D CNNs," *J. Appl. Res. Technol.*, vol. 11, no. 1, pp. 26-41, 2013.
- [18] E. Tlelo-Cuautle et al., "Frequency scaling simulation of Chua's circuit by automatic determination and control of step-size," *Appl. Math. Comput.*, vol. 194, pp. 486-491, 2007.

- [19] Z. Galias, "The dangers of rounding errors for simulations and analysis of nonlinear circuits and systems and how to avoid them," *IEEE Circuits Syst. Mag.*, vol. 13, no. 3, pp. 35-52, 2013
- [20] P.A. López and R. Aguilar, "Dynamic nonlinear feedback for temperature control of continuous stirred reactor with complex behavior," *J. Appl. Res. Technol.*, vol. 7, no. 2, pp. 202-217, 2009.
- [21] L. Gámez-Guzmán et al., "Synchronization of Chua's circuits with multi-scroll attractors: Application to communication," *Commun. Nonlinear Sci. Numer. Simul.*, vol. 14, pp. 2765–2775, 2009.
- [22] D. Chen et al., "Application of Takagi–Sugeno fuzzy model to a class of chaotic synchronization and anti-synchronization," *Nonlinear Dyn.*, vol. 73, no. 3, pp. 1495-1505, 2013.
- [23] X. Shi and Z. Wang, "The alternating between complete synchronization and hybrid synchronization of hyperchaotic Lorenz system with time delay," *Nonlinear Dyn.*, vol. 69, no. 3, pp. 1177-1190, 2012.
- [24] M. Zapateiro et al., "A secure communication scheme based on chaotic Duffing oscillators and frequency estimation for the transmission of binary-coded messages," *Commun. Nonlinear Sci. Numer. Simul.*, vol. 19, no. 4, pp. 991-1003, 2014.
- [25] E. Mahmoud, "Complex complete synchronization of two nonidentical hyperchaotic complex nonlinear systems," *Math. Meth. Appl. Sci.*, vol. 37, no. 3, pp. 321-328, 2014.
- [26] N. Bezzo et al., "Decentralized identification and control of networks of coupled mobile platforms through adaptive synchronization of chaos," *Phys. D - Nonlinear Phenomena*, vol. 267, pp. 94-103, 2014.